Hindawi
Shock and Vibration
Volume 2018, Article ID 7849153, 9 pages
https://doi.org/10.1155/2018/7849153

Research Article

Topology Optimization of Constrained Layer Damping Structures Subjected to Stationary Random Excitation

Zhanpeng Fang, Junjian Hou, and Hongfei Zhai

Henan Key Laboratory of Intelligent Manufacturing of Mechanical Equipment, Zhengzhou University of Light Industry, Zhengzhou 450002, China

Correspondence should be addressed to Zhanpeng Fang; 2015073@zzuli.edu.cn and Junjian Hou; houjunjian@zzuli.edu.cn

Received 9 May 2018; Revised 23 July 2018; Accepted 13 August 2018; Published 10 September 2018

Academic Editor: Marco Gherlone

This paper deals with an optimal layout design of the constrained layer damping (CLD) treatment of vibrating structures subjected to stationary random excitation. The root mean square (RMS) of random response is defined as the objective function as it can be used to represent the vibration level in practice. To circumvent the computationally expensive sensitivity analysis, an efficient optimization procedure integrating the pseudoexcitation method (PEM) and the double complex modal superposition method is introduced into the dynamic topology optimization. The optimal layout of CLD treatment is obtained by using the method of moving asymptote (MMA). Numerical examples are given to demonstrate the validity of the proposed optimization procedure. The results show that the optimized CLD layouts can effectively reduce the vibration response of the structures subjected to stationary random excitation.

1. Introduction

Attenuation of unwanted vibrations is important in engineering structures as they could have detrimental effects on structural performances. Constrained layer damping (CLD) treatment is an effective way to suppress structural vibrations. It is used in some critical thin-walled structures of many engineering fields including vehicles, airplanes, and ships. However, increasing the amount of CLD reduces the cost-effectiveness and increases the weight of the devices. Thus, there is a growing demand for optimizing the layout of CLD materials.

Topology optimization of the damping materials by using a modal loss factor as the objective function has attracted interests of many researchers. Zheng et al. [1] used topology optimization as a tool to optimize the CLD layouts and defined a combination of several modal loss factors solved by the finite element-modal strain energy (FE-MSE) method as the objective function. Moita et al. [2] presented an efficient finite element model for optimizing the damping of multilayer sandwich plates. The optimization is conducted in order to maximize the fundamental modal loss factor. Madeira et al. [3, 4] proposed a multiobjective method to optimize the viscoelastic laminated sandwich structures for minimizing the weight and maximizing the modal loss factors. Ansari et al. [5] adopted a level set method to search the best shapes and locations of the CLD patches on a cantilever plate for maximizing the structural modal loss factor. The result shows that the proposed method can increase the structural modal loss factor significantly through the shape change from a square to a circle. Sun et al. [6] compared the modal loss factors of the structures with damping material treatment obtained by topology optimization to the ones obtained by other approaches. The result shows that topology optimization provides about up to 61.14% higher modal loss factor. Chen and Liu [7] investigated the effect of shear modulus on the modal loss factor and optimized the microstructures of cellular viscoelastic materials with a prescribed shear modulus to improve damping. Alfouneh and Tong [8] presented a study on maximizing single and multiple modal damping ratios by finding the optimal layouts of damping layer materials and

base materials by using an extended moving isosurface threshold (MIST) topology optimization. Xu et al. [9] implemented the evolutionary structural optimization (ESO) method to optimize the layouts of the damping material attached to the headstock. The optimization results indicate that the first two orders of the modal loss factor decrease by less than 23.5% compared to the original structure when the added weight of the damping material decreases by 50%.

Many studies have recently been carried out on frequency response-based optimization of the structure with CLD treatment. Kang et al. [10] investigated the optimal distribution of the damping material in vibrating structures subject to harmonic excitations. The optimization objective function is to minimize the structural vibration at specified positions, and the steady-state response of the vibrating structure is obtained by using the complex mode superposition method in the state space to deal with the nonproportional damping. Zhang and Kang [11] proposed an optimization methodology based on the frequency response analysis, and they extended their work to simultaneous optimization of the damping and host layers. Fang and Zheng [12] proposed a topology optimization method to minimize the resonant response of plates with CLD treatment at specified broadband harmonic excitations and studied the effect of the modal sensitivity analysis on optimization of the damping material. Takezawa et al. [13] proposed complex dynamic compliance as the objective function for optimizing damping materials to reduce the resonance peak response in the frequency response problem. Zhang et al. [14] established an acoustic topology optimization model with the objective to minimize sound radiation power at a specific modal frequency.

The nature of the dynamic environment in which the real structures operate is often uncertain. The uncertain dynamic loading can be characterized as a random process, such as flying aircraft, automobile suspension systems, moving high-velocity trains, ship hulls, submarines, etc. Only a limited number of works have been devoted to the topology optimization of the structures with random excitation. Rong et al. [15] used the ESO method and the sequential quadratic programming (SQP) method to optimize continuum structures under random excitations. Zhang et al. [16] investigated the optimal placements of the components and the configuration of the structure to improve the structural static and random dynamic responses simultaneously. All the above works were carried out by using the complete quadratic combination (CQC) method. Lin et al. [17] adopted the pseudoexcitation method (PEM) as an efficient optimization procedure to optimize the piezoelectric energy harvesting devices under stationary random excitation. Zhang et al. [18] used an efficient optimization procedure integrating the pseudoexcitation method and mode acceleration method to optimize the large-scale structures subjected to stationary random excitation.

The sensitivity analysis of frequency response plays a major role in topology optimization because most frequency response-based optimizations require this information. The optimization efficiency is dependent largely on the calculating efficiency of the sensitivity analysis. Because of the CLD structure with nonviscous damping, the sensitivity analysis of frequency response is much more complicated and time consuming. It is necessary to propose an efficient sensitivity analysis method for optimizing the layout of the CLD structures subjected to stationary random excitation.

In this paper, the objective is to provide a topology optimization method to minimize the root mean square (RMS) of the CLD structures subjected to stationary random excitation. The optimization procedure integrating the PEM and the double complex modal superposition method is proposed to calculate the sensitivities of the optimization objective in order to improve the calculative efficiency. The method of moving asymptote (MMA) is adopted to search the optimal layout of CLD treatment.

2. Dynamic Responses of CLD Structure under Stationary Random Excitation

The CLD structure consists of a base plate covered with a viscoelastic material and constrained layer material. The base plate and the constrained layer are isotropic and linearly elastic, and their shear strains are negligible. The viscoelastic material dissipates the vibrational energy. The modulus of elasticity of the viscoelastic material is complex such that $E_v = E_0(1 + j\eta)$, where η is the loss factor of the viscoelastic material and $j = \sqrt{-1}$. Then, by using the finite element method, the governing equation for the structure under stationary random force excitation is written as [19]

$$\mathbf{M}\ddot{x} + (\mathbf{K}_R + j\mathbf{K}_I)\mathbf{x} = f, \tag{1}$$

where $\mathbf{M}$ is the global mass matrix, $\mathbf{K}_R$ and $\mathbf{K}_I$ are the real and imaginary parts of the stiffness matrix, and $\mathbf{x}$ is the nodal displacement vector. f is the stationary stochastic excitation force with power spectrum density (PSD) matrix $\mathbf{S}_{ff}$.

The CQC is the well-known method for solving Equation (1), and it is used to optimize the structures under random excitations. However, the CQC is not only computationally expensive but also has low computing accuracy for large-scale problems. The PEM is also known as the fast CQC. Although both methods can completely achieve the same precision with the same number of structural modes, the efficiency of the PEM is much higher than that of the CQC [20]. In this paper, the dynamic responses of the CLD structure under stationary random excitation are solved by using the PEM.

Constituting the pseudoexcitation $\tilde{f} = \mathbf{l}\sqrt{\mathbf{S}_{ff}}e^{j\omega t}$ and substituting it into Equation (1) yield

$$\mathbf{M}\ddot{\tilde{x}} + (\mathbf{K}_R + j\mathbf{K}_I)\tilde{\mathbf{x}} = \mathbf{l}\sqrt{\mathbf{S}_{ff}}e^{j\omega t}, \tag{2}$$

where $\mathbf{l}$ is a transformation matrix representing the force distribution.

The steady state pseudodisplacement response of Equation (2) can be assumed to be

$$\tilde{\mathbf{x}} = \tilde{\mathbf{X}} e^{j\omega t}. \tag{3}$$

Substituting Equation (17) into Equation (16) yields

$$\left(\mathbf{K}_{\mathrm{R}} + j\mathbf{K}_{\mathrm{I}} - \mathbf{M}\omega^2\right)\tilde{\mathbf{X}} = \tilde{\mathbf{F}}, \tag{4}$$

where $\tilde{\mathbf{F}} = \mathbf{l}\sqrt{\mathbf{S}_{\mathrm{ff}}}$.

The pseudodisplacement response can be obtained by using the complex mode superposition method:

$$\tilde{\mathbf{X}} = \sum_{r=1}^{n} \frac{\varphi_r^{\mathrm{T}} \tilde{\mathbf{F}} \varphi_r}{\omega_r^2 - \omega^2}, \tag{5}$$

where φ_r and ω_r are the complex eigenvector and complex circular eigenfrequency of the rth modal, respectively.

The pseudodisplacement $\tilde{\mathbf{X}}$ is complex, which is defined as

$$\tilde{\mathbf{X}} = \tilde{\mathbf{X}}_{\mathrm{R}} + j\tilde{\mathbf{X}}_{\mathrm{I}}, \tag{6}$$

where $\tilde{\mathbf{X}}_{\mathrm{R}}$ and $\tilde{\mathbf{X}}_{\mathrm{I}}$ are the real part and imaginary part of $\tilde{\mathbf{X}}$, respectively.

According to the PEM, the PSD of the ith degree of freedom stochastic displacement can be calculated as follows:

$$S_{x_i x_i} = \tilde{x}_i^* \tilde{x}_i^{\mathrm{T}} = \tilde{X}_{\mathrm{R}i}^2 + \tilde{X}_{\mathrm{I}i}^2. \tag{7}$$

The root mean square (RMS) can be defined as

$$\nu_{x_i x_i} = \sqrt{\int_{\omega_\alpha}^{\omega_\beta} S_{x_i x_i}\, d\omega}, \tag{8}$$

where $[\omega_\alpha, \omega_\beta]$ refers to the frequency interval of random excitation.

3. Topology Optimization

3.1. Formulation of the Optimization Problem. The RMS of random response at specified positions can be used to represent the vibration level in practice. In this way, minimizing the RMS of random displacement response at specified positions is selected as the optimization objective when the CLD structures are subjected to stationary stochastic excitations. At the same time, many engineering applications require the control of the added weight to the structures, so the consumption of the CLD material is limited strictly. Therefore, the optimization model of the problem can be described as follows:

$$\begin{cases} \text{find: } \rho_e, \quad e = 1, 2, \ldots, n, \\ \text{min: } \nu_{x_i x_i}, \\ \text{s.t.: } \dfrac{\sum_{e=1}^{n} \rho_e V_e}{\sum_{e=1}^{n} V_e} \le V^*, \\ 0 < \rho_{\min} \le \rho_e \le 1, \quad e = 1, 2, \ldots, n, \end{cases} \tag{9}$$

where ρ_e is the relative density of e element of the CLD material attached to the base plate and it is assigned as a design variable. $\rho_{\min}$ denotes the lower bound limit of the density variable, which is set to be 0.001 in this paper. ν_{xixi} is the RMS of the random displacement response of the concerned ith degree of freedom of the structure. V_e is the volume of the eth CLD element when $\rho_e = 1$. V^* is the total volume fraction ratio of the CLD material. n is the number of elements in the design domain.

3.2. The Sensitivity Analysis. The optimization problem in Equation (9) can be solved using gradient based optimization algorithms. The first-order sensitivity analysis of the RMS with respect to the design variable is presented below,

$$\frac{\partial \nu_{x_i x_i}}{\partial \rho_e} = \frac{1}{2\sigma_{x_i x_i}} \int_{\omega_\alpha}^{\omega_\beta} \frac{\partial S_{x_i x_i}}{\partial \rho_e}\, d\omega. \tag{10}$$

According to Equation (7), the following equation holds:

$$\frac{\partial S_{x_i x_i}}{\partial \rho_e} = 2\left(\tilde{\mathbf{X}}_{\mathrm{R}i} \frac{\partial \tilde{\mathbf{X}}_{\mathrm{R}i}}{\partial \rho_e} + \tilde{\mathbf{X}}_{\mathrm{I}i} \frac{\partial \tilde{\mathbf{X}}_{\mathrm{I}i}}{\partial \rho_e}\right). \tag{11}$$

The first partial derivative of Equation (4) with respect to the design variable ρ_e is presented:

$$\left(\mathbf{K}_{\mathrm{R}} + j\mathbf{K}_{\mathrm{I}} - \mathbf{M}\omega^2\right) \frac{\partial \tilde{\mathbf{X}}}{\partial \rho_e} = \mathbf{Q}, \tag{12}$$

where $\mathbf{Q}$ is defined as

$$\mathbf{Q} = -\left(\frac{\partial \mathbf{K}_{\mathrm{R}}}{\partial \rho_e} + j\frac{\partial \mathbf{K}_{\mathrm{I}}}{\partial \rho_e} - \omega^2 \frac{\partial \mathbf{M}}{\partial \rho_e}\right)\tilde{\mathbf{X}}. \tag{13}$$

The sensitivities of the pseudodisplacement response can be obtained by using the double complex modal superposition method, which are defined as

$$\frac{\partial \tilde{\mathbf{X}}}{\partial \rho_e} = \sum_{r=1}^{n} \frac{\varphi_r^{\mathrm{T}} \mathbf{Q} \varphi_r}{\omega_r^2 - \omega^2}. \tag{14}$$

The base plate is not changed. Based on the solid isotropic material with penalization (SIMP) method [21], the global mass and stiffness matrices can be calculated as follows:

$$\mathbf{M} = \sum_{e=1}^{n} \left(\mathbf{M}_{\mathrm{b}}^e + \rho_e^p \left(\mathbf{M}_{\mathrm{v}}^e + \mathbf{M}_{\mathrm{c}}^e\right)\right), \tag{15}$$

$$\mathbf{K}_{\mathrm{R}} = \sum_{e=1}^{n} \left(\mathbf{K}_{\mathrm{b}}^e + \rho_e^q \left(\mathbf{K}_{\mathrm{v}}^e + \mathbf{K}_{\mathrm{c}}^e\right)\right), \tag{16}$$

$$\mathbf{K}_{\mathrm{I}} = \sum_{e=1}^{n} \rho_e^q \left(\mathbf{K}_{\mathrm{v}}^e\right)\eta. \tag{17}$$

In the above equations, $\mathbf{M}_{\mathrm{b}}^e$, $\mathbf{M}_{\mathrm{v}}^e$, $\mathbf{M}_{\mathrm{c}}^e$, $\mathbf{K}_{\mathrm{b}}^e$, $\mathbf{K}_{\mathrm{v}}^e$, and $\mathbf{K}_{\mathrm{c}}^e$ are the eth element mass and stiffness matrices of the base plate, VEM layer, and constrained layer, respectively. p and q are the penalty factors, with values of 1 and 3.

The sensitivities of the mass matrix and the stiffness matrix with respect to the design variables can be calculated:

$$\frac{\partial \mathbf{M}}{\partial \rho_e} = \mathbf{M}_{\mathrm{v}}^e + \mathbf{M}_{\mathrm{c}}^e,$$

$$\frac{\partial \mathbf{K}_{\mathrm{R}}}{\partial \rho_e} = q\rho_e^{q-1}\left(\mathbf{K}_{\mathrm{v}}^e + \mathbf{K}_{\mathrm{c}}^e\right), \tag{18}$$

$$\frac{\partial \mathbf{K}_{\mathrm{I}}}{\partial \rho_e} = q\rho_e^{q-1}\mathbf{K}_{\mathrm{v}}^e \eta.$$

3.3. Optimization Strategy. The MMA is usually flexible and theoretically well found to deal with large-scale topology optimization designs with complicated objectives and multiple constraints [22]. It is widely used in topology optimization of structures [23–25]. In this paper, the MMA is used to update the design variable. The flowchart for the implementation of the topology optimization procedures is shown in Figure 1.

4. Numerical Examples

4.1. The Cantilever Plate/CLD System. A numerical example involving a cantilever plate/CLD system is provided first to confirm the validity of the proposed methodology. The cantilever plate/CLD system clamped is shown in Figure 2. It is clamped at the left side, and the stationary random excitation with PSD value 1 N^2/Hz is applied at the middle node of the right edge. The length and width of the plate/CLD system are 0.2 m and 0.1 m, respectively. The thickness of the base plate, VEM layer, and constrained layer is 0.002 m, 0.0001 m, and 0.0002 m, respectively. The material of the base layer and constrained layer is aluminum with Young's modulus of 70 GPa, Poisson's ratio of 0.3, and mass density of 2700 kg/m^3. The physical properties of the VEM layer are Young's modulus of 12 MPa, Poisson's ratio of 0.495, mass density of 1200 kg/m^3, and a loss factor of 0.5.

The location of the excitation force is always the main vibration source, and the optimization objective is to minimize the RMS of vertical displacement at the loading position. The fraction ratio of CLD V^* is restricted to 0.5. It means that the volume consumption of the CLD material is limited to 50% of full coverage after optimization. The initial values of the design variables are set to 0.5. Two frequency intervals of random force excitation are considered with $f = [0, 100]$ Hz and $f = [100, 1000]$ Hz.

The optimal layouts of CLD treatment are shown in Figure 3. The convergence histories of the objective function are plotted in Figure 4. It is noted that the objective function finally convergences to a stable value after a certain iteration number. Table 1 is the comparison of objective functions before and after optimization. It can be seen that the values of the objective function of the CLD structure are greatly decreased through optimizing the layout of the CLD treatment. The PSD curves are shown in Figure 5. It is shown that PSD curves of optimized structures globally decrease within the prescribed frequency intervals.

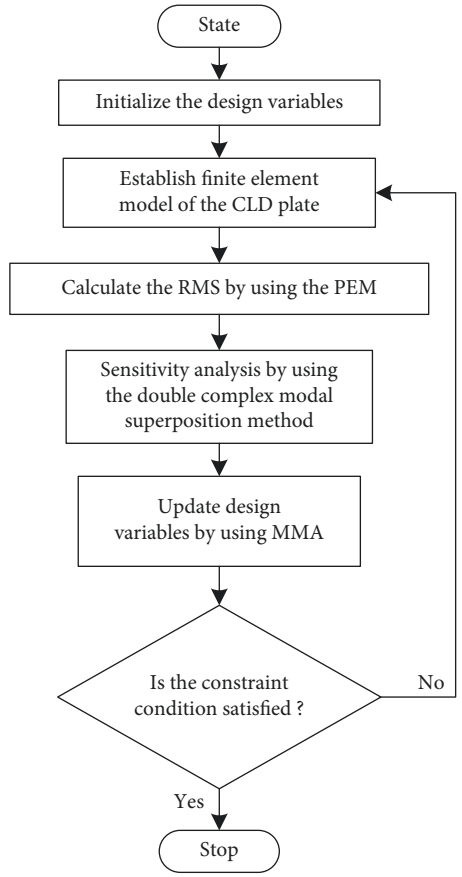

Figure 1: Block diagram of the optimization procedure.

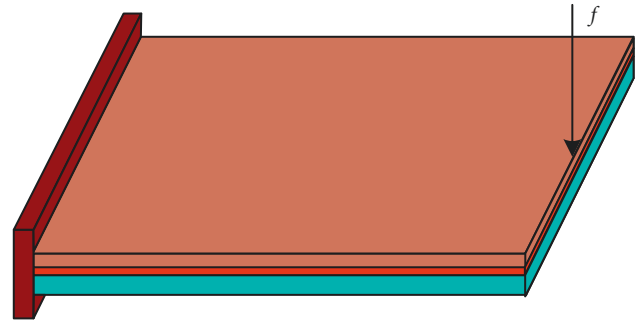

Figure 2: The cantilever plate/CLD system.

To further verify the effectiveness of the proposed optimization method, the initial values of the design variables are, respectively, set to 0.001 and 0.75. The optimal layouts of CLD treatment are shown in Figure 6. The values of the objective function of the optimal layouts of CLD treatment are shown in Table 2. For the frequency interval of random force excitation $f = [100, 1000]$ Hz, it can be seen that the optimal layouts of CLD treatment are different when the initial values of the design variables are different. This is because the MMA is used in this paper. The MMA is not a global optimization method, so it is normal to get local optima instead of global optima. It is normal to obtain different solutions when the initial values of the design variables are different.

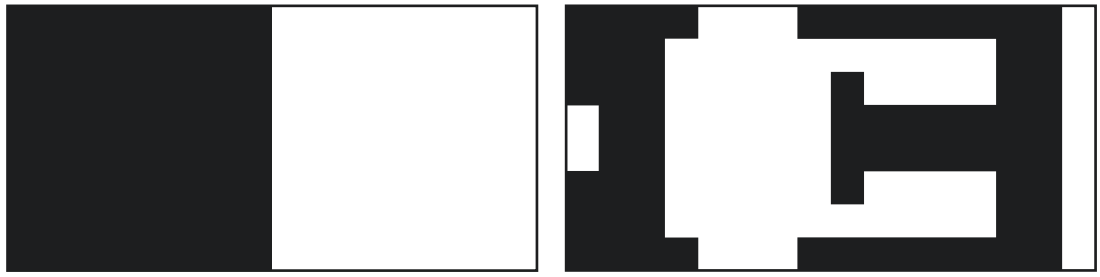

(a) (b)

Figure 3: The optimal layouts of CLD treatment. (a) $f = [0, 100]$ Hz and (b) $f = [100, 1000]$ Hz.

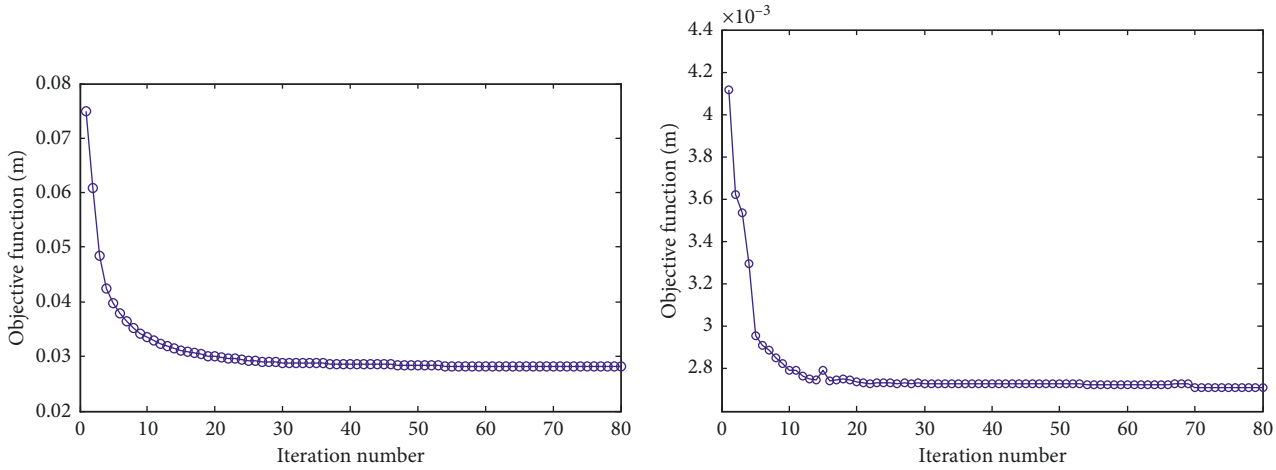

(a) (b)

Figure 4: The convergence histories of the objective function. (a) $f = [0, 100]$ Hz and (b) $f = [100, 1000]$ Hz.

Table 1: The comparison of the values of the objective function before and after optimization.

	Values of the objective function		
	Initial design (m)	Optimized structure (m)	Percentage of reduction
$f = [0, 100]$ Hz	0.074	0.0287	61.22
$f = [100, 1000]$ Hz	0.00412	0.00273	33.74

4.2. The Plate/CLD System with Two Short Edges Clamped. Figure 7 is the plate/CLD system with two short edges clamped. The length and width of the plate/CLD system are 0.4 m and 0.2 m, respectively. Other physical and geometrical parameters are the same as the first example. The stationary random excitation with PSD value 1 N^2/Hz is applied at the center of the plate. In a similar way, the minimization of the RMS of vertical displacement at the excitation point is selected as the optimization objective. The fraction ratio of CLD is restricted to 0.5. The initial values of the design variables are set to 0.5. Two frequency intervals are considered with $f = [0, 100]$ Hz and $f = [100, 1000]$ Hz.

The optimal layouts of CLD treatment are shown in Figure 8. The convergence histories of the objective function are plotted in Figure 9. It is noted that the objective function also convergences to a stable value after a certain iteration number. Table 3 is the comparison of objective functions before and after optimization. It can be seen that the objective functions of the CLD structure are greatly decreased through optimizing the layout of the CLD treatment. The PSD curves are shown in Figure 10. It is shown that the PSD is effectively attenuated by the proposed optimization method.

To further verify the effectiveness of the proposed optimization method, the initial values of the design variables are, respectively, set to 0.001 and 0.75. The optimal layouts of CLD treatment are shown in Figure 11. The values of the objective function of the optimal layouts of CLD treatment are shown in Table 4. It can be seen that the optimal layouts of CLD treatment and the values of the objective function are different when the initial values of the design variables are different. It is also because the MMA is used in this paper.

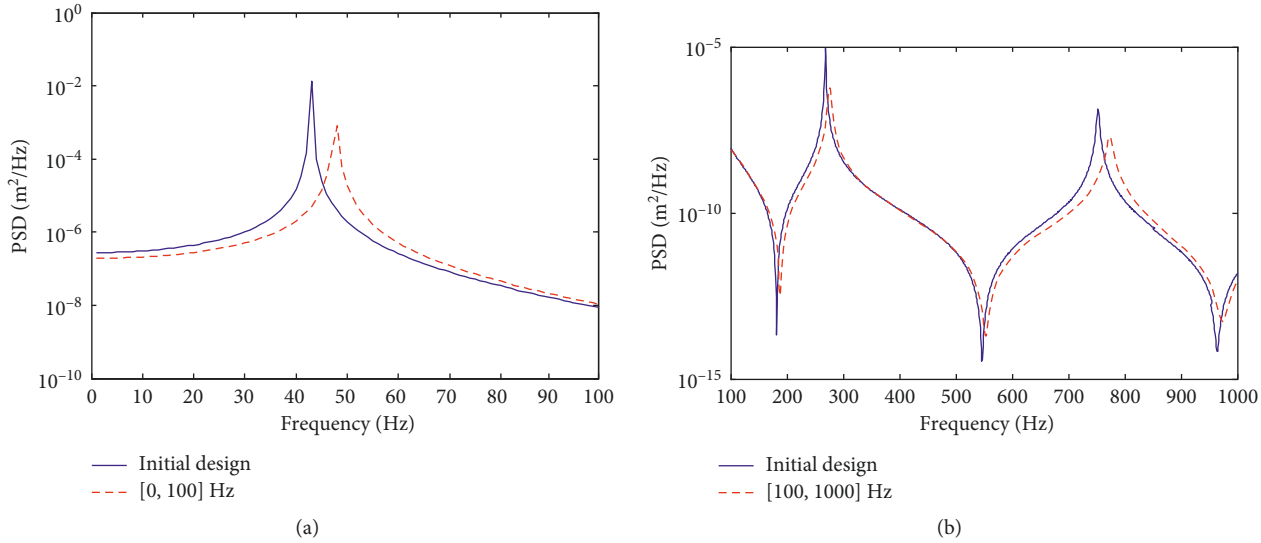

Figure 5: PSD curves of the initial and optimal design of CLD treatment. (a) $f = [0, 100]$ Hz and (b) $f = [100, 1000]$ Hz.

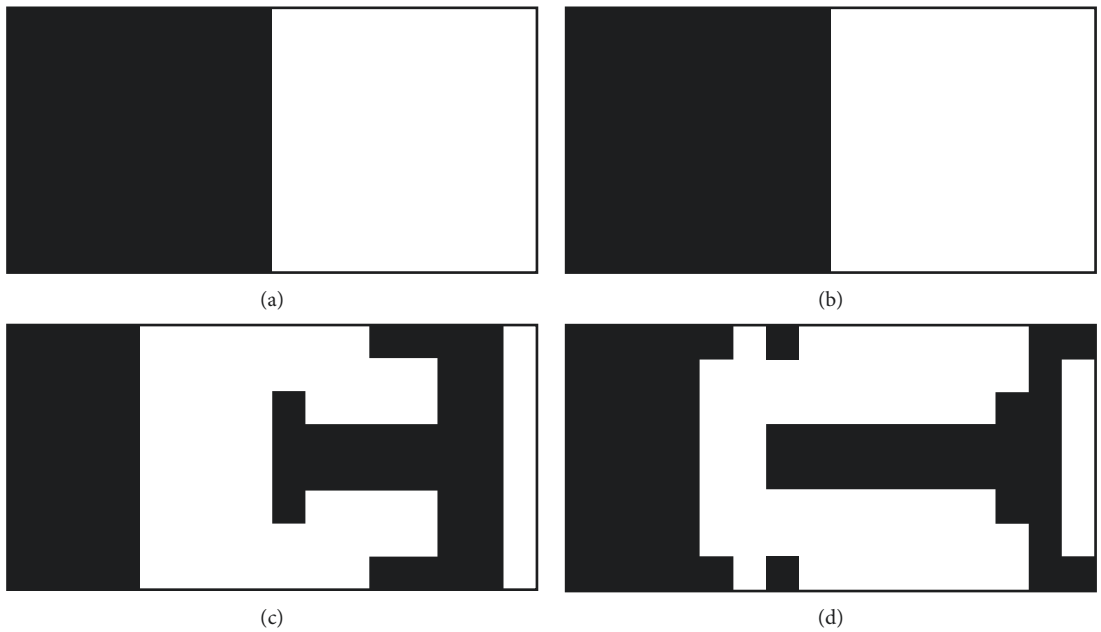

Figure 6: The optimal layouts of CLD treatment. (a) $f = [0, 100]$ Hz and the initial values of the design variables 0.001. (b) $f = [0, 100]$ Hz and the initial values of the design variables 0.75. (c) $f = [100, 1000]$ Hz and the initial values of the design variables 0.001. (d) $f = [100, 1000]$ Hz and the initial values of the design variables 0.75.

Table 2: The values of the objective function of the optimal layouts of CLD treatment.

	Values of objective function	
	Initial values of the design variable 0.001 (m)	Initial values of the design variable 0.75 (m)
$f = [0, 100]$ Hz	0.0287	0.0287
$f = [100, 1000]$ Hz	0.00284	0.00284

5. Conclusion

This work developed a topology optimization method to minimize the RMS of the CLD structures subjected to stationary random excitation. In order to improve the calculative efficiency, the PEM is introduced to analyze the dynamic responses of CLD structures under stationary random excitation and the double complex modal

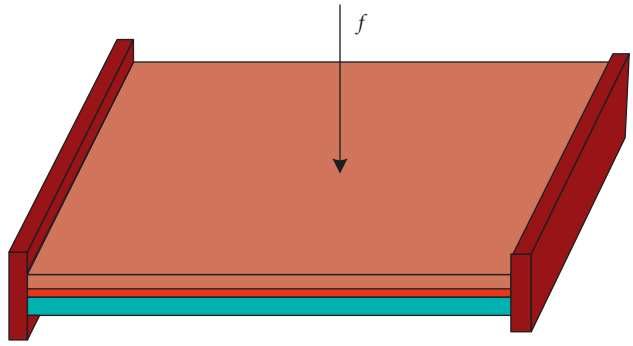

Figure 7: The plate/CLD system with two short edges clamped.

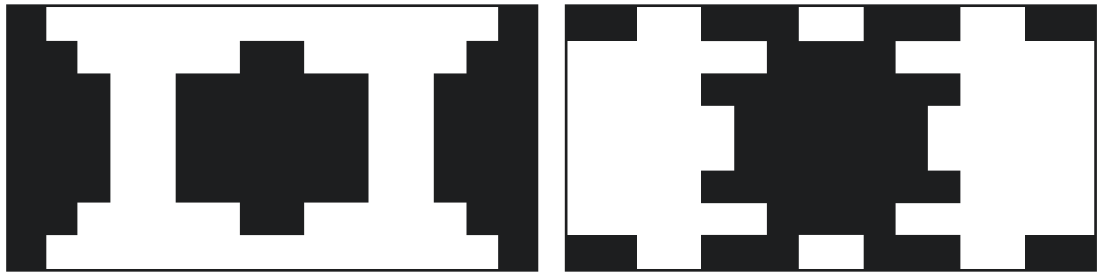

(a) (b)

Figure 8: The optimal layouts of CLD treatment. (a) $f = [0, 100]$ Hz and (b) $f = [100, 1000]$ Hz.

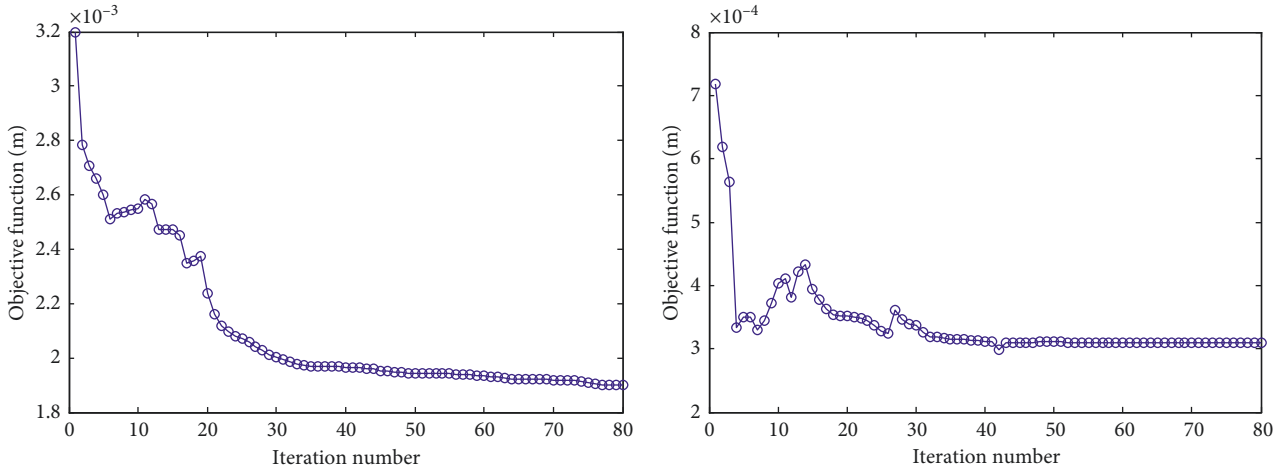

(a) (b)

Figure 9: The convergence histories of the objective function. (a) $f = [0, 100]$ Hz and (b) $f = [100, 1000]$ Hz.

Table 3: The comparison of objective functions before and after optimization.

	Value of objective function		
	Initial design (m)	Optimized structure (m)	Percentage of reduction
$f = [0, 100]$ Hz	0.0032	0.0019	40.63
$f = [100, 1000]$ Hz	0.00071	0.000305	57.04

superposition method is used to calculate the sensitivities of the RMS. The numerical examples demonstrated the effectiveness of the proposed method. It can be very useful in the design of this kind of structures, where the PSD of optimized structures globally decrease within the prescribed frequency intervals.

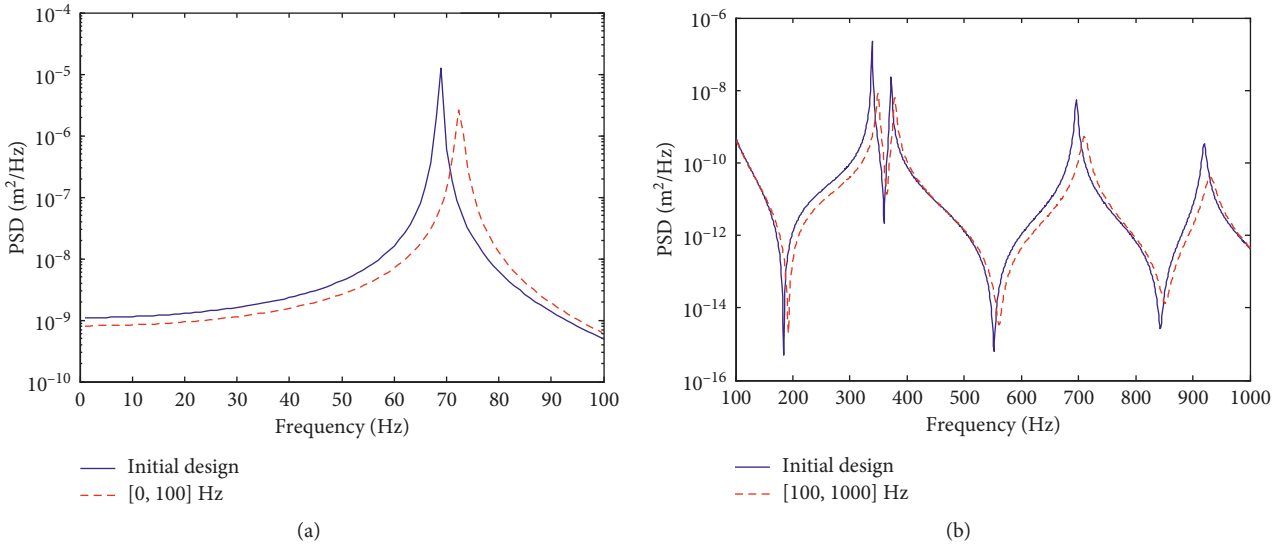

Figure 10: PSD curves of the initial and optimal design of CLD treatment. (a) $f = [0, 100]$ Hz and (b) $f = [100, 1000]$ Hz.

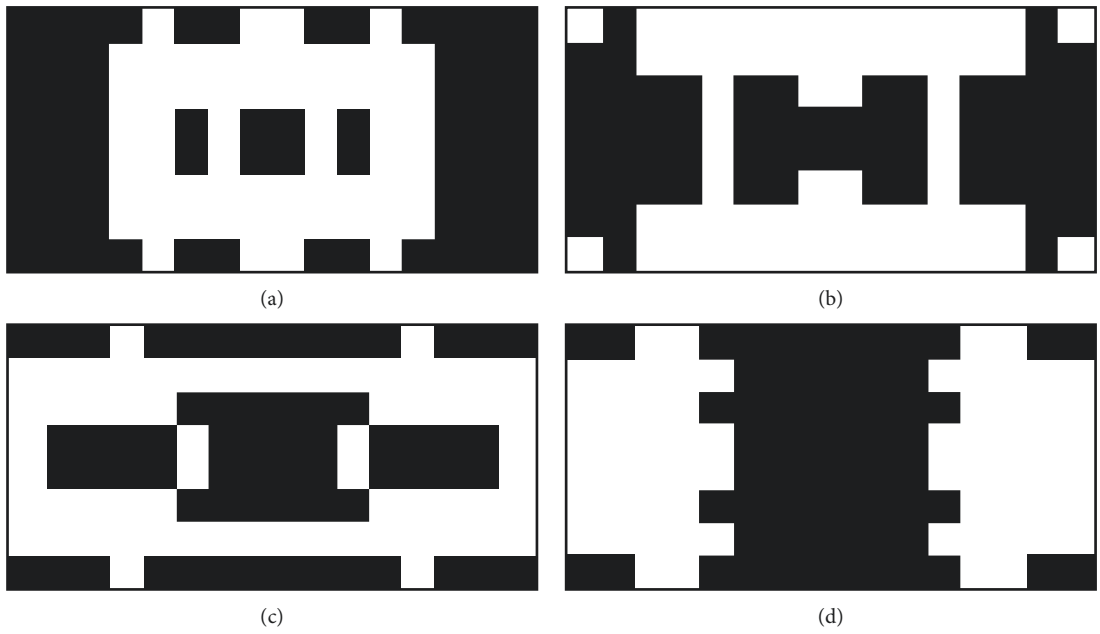

Figure 11: The optimal layouts of CLD treatment. (a) $f = [0, 100]$ Hz and the initial values of the design variables 0.001. (b) $f = [0, 100]$ Hz and the initial values of the design variables 0.75. (c) $f = [100, 1000]$ Hz and the initial values of the design variables 0.001. (d) $f = [100, 1000]$ Hz and the initial values of the design variables 0.75.

Table 4: The values of the objective function of the optimal layouts of CLD treatment.

	Values of the objective function	
	Initial values of the design variable 0.001 (m)	Initial values of the design variable 0.75 (m)
$f = [0, 100]$ Hz	0.0020	0.0021
$f = [100, 1000]$ Hz	0.000263	0.000312

Data Availability

The data used to support the findings of this study are available from the corresponding author upon request.

Conflicts of Interest

The authors declare that they have no conflicts of interest.

Acknowledgments

This project was supported by the Natural Science Foundation of China (Grant nos. 51805491 and 50775225), the Plan of Key Research Projects of Higher Education of Henan Province (Grant no. 16A460028), and the Project of Science and Technology of Henan Province (Grant no. 172102210058).

References

[1] W. Zheng, Y. Lei, S. Li, Q. Huang, and W. Zheng, "Topology optimization of passive constrained layer damping with partial coverage on plate," *Shock and Vibration*, vol. 20, no. 2, pp. 199–211, 2015.

[2] J. S. Moita, C. M. M. Soares, and C. A. M. Soares, "Finite element model for damping optimization of viscoelastic sandwich structures," *Advances in Engineering Software*, vol. 66, no. 4, pp. 34–39, 2013.

[3] J. F. A. Madeira, A. L. Araújo, C. M. Mota Soares, C. A. Mota Soares, and A. J. M. Ferreira, "Multiobjective design of viscoelastic laminated composite sandwich panels," *Composites Part B: Engineering*, vol. 77, pp. 391–401, 2015.

[4] R. T. Marler and J. S. Arora, "Survey of multi-objective optimization methods for engineering," *Structural and Multidisciplinary Optimization*, vol. 26, no. 6, pp. 369–395, 2004.

[5] M. Ansari, A. Khajepour, and E. Esmailzadeh, "Application of level set method to optimal vibration control of plate structures," *Journal of Sound and Vibration*, vol. 332, no. 4, pp. 687–700, 2013.

[6] Y. K. Sun, C. K. Mechefske, and I. Y. Kim, "Optimal damping layout in a shell structure using topology optimization," *Journal of Sound and Vibration*, vol. 332, no. 12, pp. 2873–2883, 2013.

[7] W. Chen and S. Liu, "Topology optimization of microstructures of viscoelastic damping materials for a prescribed shear modulus," *Structural and Multidisciplinary Optimization*, vol. 50, no. 2, pp. 287–296, 2014.

[8] M. Alfouneh and L. Tong, "Maximizing modal damping in layered structures via multi-objective topology optimization," *Engineering Structures*, vol. 132, pp. 637–647, 2017.

[9] Y. Xu, W. Gao, Y. Yu et al., "Dynamic optimization of constrained layer damping structure for the headstock of machine tools with modal strain energy method," *Shock and Vibration*, vol. 10, Article ID 2736545, 13 pages, 2017.

[10] Z. Kang, X. Zhang, S. Jiang, and G. Cheng, "On topology optimization of damping layer in shell structures under harmonic excitations," *Structural and Multidisciplinary Optimization*, vol. 46, no. 1, pp. 51–67, 2012.

[11] X. Zhang and Z. Kang, "Vibration suppression using integrated topology optimization of host structures and damping layers," *Journal of Vibration and Control*, vol. 22, no. 1, 2014.

[12] Z. Fang and L. Zheng, "Topology optimization for minimizing the resonant response of plates with constrained layer damping treatment," *Shock and Vibration*, vol. 2015, Article ID 376854, 11 pages, 2015.

[13] A. Takezawa, M. Daifuku, Y. Nakano et al., "Topology optimization of damping material for reducing resonance response based on complex dynamic compliance," *Journal of Sound and Vibration*, vol. 365, pp. 230–243, 2016.

[14] D. Zhang, S. Wang, and L. Zheng, "A comparative study on acoustic optimization and analysis of a CLD/plate in a cavity using ESO and GA," *Shock and Vibration*, vol. 2018, Article ID 7146580, 16 pages, 2018.

[15] J. H. Rong, Z. L. Tang, Y. M. Xie, and F. Y. Li, "Topological optimization design of structures under random excitations using SQP method," *Engineering Structures*, vol. 56, no. 6, pp. 2098–2106, 2013.

[16] Z. Qiao, Z. Weihong, Z. Jihong, and G. Tong, "Layout optimization of multi-component structures under static loads and random excitations," *Engineering Structures*, vol. 43, no. 43, pp. 120–128, 2012.

[17] Z. Q. Lin, H. C. Gea, and S. T. Liu, "Design of piezoelectric energy harvesting devices subjected to broadband random vibrations by applying topology optimization," *Acta Mechanica Sinica*, vol. 27, no. 5, pp. 730–737, 2011.

[18] W. Zhang, H. Liu, and T. Gao, "Topology optimization of large-scale structures subjected to stationary random excitation: an efficient optimization procedure integrating pseudo excitation method and mode acceleration method," *Computers and Structures*, vol. 158, pp. 61–70, 2015.

[19] Z. Ling, X. Ronglu, W. Yi, and A. El-Sabbagh, "Topology optimization of constrained layer damping on plates using method of moving asymptote (MMA) approach," *Shock and Vibration*, vol. 18, no. 1-2, pp. 221–244, 2011.

[20] J. Lin, Y. Zhao, and Y. Zhang, "Accurate and highly efficient algorithms for structural stationary/non-stationary random responses," *Computer Methods in Applied Mechanics and Engineering*, vol. 191, no. 1-2, pp. 103–111, 2001.

[21] M. P. Bendsøe, "Optimal shape design as a material distribution problem," *Structural Optimization*, vol. 1, pp. 193–202, 1989.

[22] K. Svanberg, "The method of moving asymptotes—a new method for structural optimization," *International Journal for Numerical Methods in Engineering*, vol. 24, no. 2, pp. 359–373, 1987.

[23] J. Zhao and C. Wang, "Topology optimization for minimizing the maximum dynamic response in the time domain using aggregation functional method," *Computers and Structures*, vol. 190, pp. 41–60, 2017.

[24] J. Kook and J. S. Jensen, "Topology optimization of periodic microstructures for enhanced loss factor using acoustic–structure interaction," *International Journal of Solids and Structures*, vol. 122, no. 123, pp. 59–68, 2017.

[25] K. S. Yun and S. K. Youn, "Multi-material topology optimization of viscoelastically damped structures under time-dependent loading," *Finite Elements in Analysis and Design*, vol. 123, pp. 9–18, 2017.